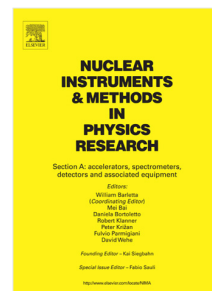


Journal Pre-proof

Application of compact laser-driven accelerator X-ray sources for industrial imaging

J.-N. Gruse, M.J.V. Streeter, C. Thornton, C.D. Armstrong, C.D. Baird, N. Bourgeois, S. Cipiccia, O.J. Finlay, C.D. Gregory, Y. Katzir, N.C. Lopes, S.P.D. Mangles, Z. Najmudin, D. Neely, L.R. Pickard, K.D. Potter, P.P. Rajeev, D.R. Rusby, C.I.D. Underwood, J.M. Warnett, M.A. Williams, J.C. Wood, C.D. Murphy, C.M. Brenner, D.R. Symes



PII: S0168-9002(20)30766-X
DOI: <https://doi.org/10.1016/j.nima.2020.164369>
Reference: NIMA 164369

To appear in: *Nuclear Inst. and Methods in Physics Research, A*

Received date: 30 April 2020

Revised date: 10 July 2020

Accepted date: 13 July 2020

Please cite this article as: J.-N. Gruse, M.J.V. Streeter, C. Thornton et al., Application of compact laser-driven accelerator X-ray sources for industrial imaging, *Nuclear Inst. and Methods in Physics Research, A* (2020), doi: <https://doi.org/10.1016/j.nima.2020.164369>.

This is a PDF file of an article that has undergone enhancements after acceptance, such as the addition of a cover page and metadata, and formatting for readability, but it is not yet the definitive version of record. This version will undergo additional copyediting, typesetting and review before it is published in its final form, but we are providing this version to give early visibility of the article. Please note that, during the production process, errors may be discovered which could affect the content, and all legal disclaimers that apply to the journal pertain.

© 2020 Published by Elsevier B.V.

1 Highlights

2 **Application of Compact Laser-Driven Accelerator X-Ray Sources for Industrial Imaging**

3 J.-N. Gruse, M. J. V. Streeter, C. Thornton, C. D. Armstrong, C. D. Baird, N. Bourgeois, S. Cipiccia, O. J. Finlay, C. D.
4 Gregory, Y. Katzir, N. C. Lopes, S. P. D. Mangles, Z. Najmudin, D. Neely, L. R. Pickard, K. D. Potter, P. P. Rajeev, D. R.
5 Rusby, C. I. D. Underwood, J. M. Warnett, M. A. Williams, J. C. Wood, C. D. Murphy, C. M. Brenner, D. R. Symes

- 6 • Laser plasma wakefield acceleration produced high X-ray yield
- 7 • Radiographs were produced of a metrology test sample, battery electrodes, and a damage site in a composite
8 material
- 9 • This novel method is shown to produce image quality comparable, if not better, than industrial standards

Application of Compact Laser-Driven Accelerator X-Ray Sources for Industrial Imaging

J.-N. Gruse^{a,*}, M. J. V. Streeter^{a,e}, C. Thornton^b, C. D. Armstrong^b, C. D. Baird^{b,d},
 N. Bourgeois^b, S. Cipiccia^f, O. J. Finlay^e, C. D. Gregory^b, Y. Katzir^b, N. C. Lopes^{a,c}, S. P.
 D. Mangles^a, Z. Najmudin^a, D. Neely^b, L. R. Pickard^g, K. D. Potter^h, P. P. Rajeev^b, D.
 R. Rusby^{b,1}, C. I. D. Underwood^d, J. M. Warnettⁱ, M. A. Williamsⁱ, J. C. Wood^{a,2}, C.
 D. Murphy^d, C. M. Brenner^b and D. R. Symes^b

^aJohn Adams Institute for Accelerator Science, Imperial College London, London, SW7 2BZ, UK

^bCentral Laser Facility, STFC Rutherford Appleton Laboratory, OX11 0QX, UK

^cGoLP, IPFN, Instituto Superior Tecnico, U. Lisboa, Portugal

^dYork Plasma Institute, Department of Physics, University of York, York YO10 5DD, UK

^ePhysics Department, Lancaster University, Lancaster LA1 4YB, UK

^fDiamond Light Source, Harwell Science & Innovation Campus, Oxfordshire OX11 0DE, UK

^gNational Composites Centre, Bristol and Bath Science Park, Feynman Way Central, Emersons Green, Bristol BS16 7FS, UK

^hAdvanced Composites Collaboration for Science and Innovation (ACCIS) University of Bristol, Bristol BS8 1TR, UK

ⁱWMG, University of Warwick, Coventry CV4 7AL, UK

ARTICLE INFO

Keywords:

LPWA

Betatron radiation

Radiographs

Novel Industrial x-ray Imaging

Femto-second x-ray Imaging

ABSTRACT

X-rays generated by betatron oscillations of electrons in a laser-driven plasma accelerator were characterised and applied to imaging industrial samples. With a 125 TW laser, a low divergence beam with $7.5 \pm 2.6 \times 10^8$ photons mrad^{-2} per pulse was produced with a synchrotron spectrum with a critical energy of 14.6 ± 1.3 keV. Radiographs were obtained of a metrology test sample, battery electrodes, and a damage site in a composite material. These results demonstrate the suitability of the source for non-destructive evaluation applications. The potential for industrial implementation of plasma accelerators is discussed.

1. Introduction

Advances in industrial methods, such as additive manufacturing (AM), are enabling the fabrication of better and more complicated products than are achievable with traditional manufacturing. Environmental sustainability is a major incentive to develop less wasteful processes, new materials, and energy storage solutions. For example, many aircraft and automotive components are now produced using lightweight fibre reinforced composites to improve fuel efficiency. In parallel, the more widespread adoption of electric vehicles is driving investment and innovation in battery technologies. Rapid growth in these sectors means that in some cases demand is outstripping supply and there is a need for industry to increase productivity. Progress in manufacturing needs to be accompanied by improvements in

*Corresponding author

 j.gruse16@imperial.ac.uk (J.-N. Gruse)

ORCID(s): 0000-0002-4099-8341 (J.-N. Gruse)

¹Now: Lawrence Livermore National Laboratory, Livermore, California 94550, USA

²Now: Deutsches Elektronen-Synchrotron (DESY), Notkestrasse 85, Hamburg, Germany

Application of Compact Laser-Driven Accelerator X-Ray Sources for Industrial Imaging

the product inspection tools employed for metrology and quality control. X-ray computed tomography (XCT) is a powerful technique because it allows non-destructive evaluation (NDE) of the internal structure of dense objects. XCT is generally conducted using commercial x-ray tubes and linear accelerators but for some applications these sources are not able to simultaneously meet the demanding requirements on penetration, scan speed and spatial resolution³. Superior imaging capability can be achieved using synchrotron light sources, but these are national-scale facilities which are in high demand so that access for industrial inspection is limited.

We present an alternative compact, laser-based light source for industrial inspection that delivers extreme brightness, ultrashort x-ray pulses. This synchrotron source relies on a plasma-based electron accelerator driven by a high power laser (> 100 TW) [1]. The laser pulse is focused on to a gas target at a high intensity of 10^{19} W cm⁻², expelling on-axis electrons and creating ion cavities in its wake. Electrons injected into a cavity are subject to strong transverse and longitudinal electric fields (~ 100 GeV m⁻¹), accelerating to energies of multiple GeV within centimetres [2] and emitting on-axis betatron radiation as they oscillate [3, 4]. For electrons with energy $\gamma m_e c^2$, the characteristics of the radiation are determined by the wiggler strength parameter $\alpha_\beta = \gamma k_\beta r_\beta$, where r_β is the amplitude and $k_\beta = 2\pi/\lambda_\beta$ is the wavenumber associated with betatron oscillations of wavelength λ_β . For self-injected electron bunches, where the accelerated electrons are swept up from the plasma itself, the parameter obeys $\alpha_\beta > 1$ and the radiation has the form of a broad band on-axis synchrotron spectrum [5, 6] with a peak close to the critical energy

$$E_{\text{crit}} = \frac{3}{2} \hbar c \alpha_\beta k_\beta \gamma^2. \quad (1)$$

The number of photons can reach 10^{10} photons per pulse in a beam with 10 mrad divergence and critical energies in the range 10 – 50 keV [7, 8], 10% stability [9] and pulse lengths of <100 fs [10, 11].

The small size of the laser-driven accelerator is a key advantage compared to conventional synchrotron light sources and the technology has the potential to be used for a broad range of applications [1]. Tomographic imaging of biological samples [7, 8, 12, 13], time resolved radiography of high energy density plasma [14] and imaging of AM objects [15] and complex microstructures [16] has been reported. The short pulse duration enables radiographic snapshots of fast moving parts with no motion blur. In addition, the source is suitable for x-ray absorption spectroscopy with exceptional time resolution [11]. Because the x-ray source size is of order of $2r_\beta \approx 1 \mu\text{m}$, high resolution imaging can be conducted with high x-ray flux, avoiding the trade off between source size and power encountered with conventional x-ray machines. Furthermore, within 1 m the beam has a transverse coherence length of $10^3 \mu\text{m}$ meaning that phase enhancement can be obtained with a compact imaging arrangement [17]. Phase contrast provides superior image quality for low density objects that only weakly attenuate x-rays and better distinction between items made of similar materials [18]. This technique has been demonstrated on biological samples using plasma based accelerators [17, 19].

³epsrc.ukri.org/files/research/epsrc-x-ray-tomography-roadmap-2018

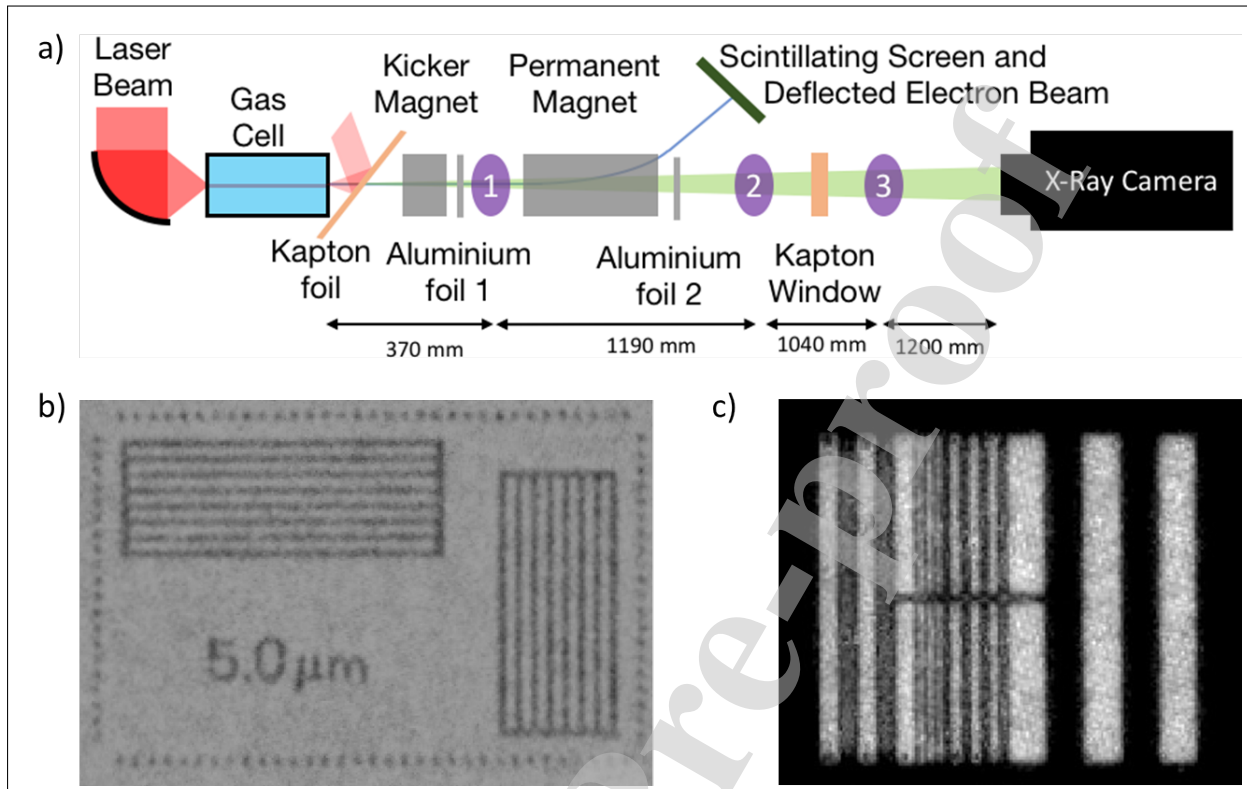


Figure 1: a) Schematic of the laser-betatron x-ray source including three sample positions (purple). The laser beam (red) is focused into a gas cell, in which electrons (blue) are accelerated, which then produce x-rays (green). Radiographs of: b) resolution target (JIMA RT RC-02) with $5\mu\text{m}$ line spacing, imaged at position 1 ($M=10.2$); c) resolution target (gold grid) with line spacing from left to right: $41.1\mu\text{m}$, $10.95\mu\text{m}$, $23.27\mu\text{m}$ and $75.3\mu\text{m}$ imaged at position 2 ($M=2.2$).

75 In this work, we demonstrate the feasibility of using laser-betatron radiation for high resolution NDE of industrially
 76 relevant components. The laser generates x-ray energies in the 10s keV range, ideal for low density polymer and
 77 carbon-fibre composite materials. We characterise the properties of the x-ray beams and present example images of
 78 samples relevant to three particular areas of importance to industry: accurate metrology, battery development and
 79 composite manufacturing. We will discuss the potential of these sources for high frame rate industrial XCT as the
 80 underpinning laser technology develops to higher repetition rate operation in the next few years.

81 2. Imaging Set-up and X-Ray Source

82 The beam line apparatus used to produce the x-ray beam can be seen in Fig. 1. The Gemini Ti:sapphire laser,
 83 providing pulses of duration 49 ± 3 fs and 7.2 ± 0.4 J on target, was focused with an off-axis $f/40$ parabola into a gas
 84 cell inside a vacuum chamber. Orthogonal to the main beam, a second laser pulse was used to measure the plasma
 85 electron density interferometrically. After the cell, the laser beam, electron beam and x-ray beam transited a $25\mu\text{m}$
 86 polyimide tape, which functioned as a plasma mirror deflecting most of the undepleted laser energy [20]. A $13\mu\text{m}$

Application of Compact Laser-Driven Accelerator X-Ray Sources for Industrial Imaging

87 aluminium foil protected the sample from any remaining laser light and also acted to filter out 93% of the energy of
 88 a 14.6 keV-synchrotron spectrum below the k-edge (1.6 keV). Electrons were deflected off axis with a permanent
 89 magnetic dipole and observed on a scintillating screen to measure their energy spectrum. The x-ray beam exited
 90 the vacuum chamber through a 250 μm polyimide window and propagated through 2050 mm of air onto an indirect
 91 detection x-ray camera. This consisted of 150 μm thick caesium-iodide scintillator fibre-coupled to a 2048 \times 2048
 92 pixel CCD (Andor *iKon-L 936*) of pixel size 13.6 μm .

93 The gas cell length and gas pressure were scanned to determine the optimal parameters for generating stable x-ray
 94 beams. The most reproducible beams with the highest x-ray flux were measured at a plasma density of $(4.4 \pm 0.4) \times 10^{18}$
 95 cm^{-3} with an average peak energy of the electrons of 435 ± 7 MeV. The corresponding plasma wave wavelength λ_p
 96 implies a maximal x-ray pulse duration $\lambda_p/c \approx 50$ fs. The x-ray spectrum was measured using 12 materials in a filter
 97 pack configuration [21]. By comparing the transmission of the different materials relative to each other and finding
 98 the best fit synchrotron spectrum, the critical energy Eq. (1) was found to be 14.6 ± 1.3 keV for photons in the range
 99 0.1 – 300 keV. The emitted x-ray flux from the source was determined to be $7.5 \pm 2.6 \times 10^8$ photons mrad^{-2} per pulse
 100 and the transverse source size was inferred from the betatron parameters to be $2 \cdot r_B = 2.3 \pm 0.3$ μm (Eq. (1)).

101 The divergence of the x-ray beam (~ 10 mrad) allows geometrical magnification. The beam line included three
 102 sample stages located at different distances in order to vary the x-ray field-of-view, as indicated in Fig. 1. Samples
 103 outside vacuum (position 3) could be positioned anywhere from the rear wall of the chamber to directly in front of the
 104 camera. Inside the vacuum chamber, a stage was placed close to the exit window (position 2) yielding a magnification
 105 $M=2.2$, well suited for cm-scale objects. The highest magnification was $M=10.2$ with the sample placed 370 mm
 106 from the source (position 1). Because this stage was located before the electron spectrometer magnet, an additional
 107 kicker magnet was inserted in this case to prevent the electron beam from striking the sample. The magnification was
 108 measured at position 1 using a JIMA *RT RC-02* resolution target and in configuration 2 using a gold foil with a pattern
 109 of horizontal and vertical apertures. The resulting radiographs are shown in Fig. 1.

110 Radiographs of industrial samples taken with the laser-betatron source are presented in Section 3. To provide context
 111 for each particular application, we also display 3D reconstructions of the same objects obtained using the commercial
 112 XCT scanners currently being used. In this work, it is not our intention to directly compare image quality between the
 113 x-ray sources. Rather, our aim is to demonstrate the capability for high quality imaging of such objects, with a view to
 114 offering advanced XCT using this technology in the future. The laser-betatron images in Figs. 2 and 3 were obtained
 115 with the samples placed outside the vacuum chamber with magnification of $M=1.5$; the sample shown in Fig. 4 was
 116 imaged at position 2 ($M=2.2$). The image resolution was detector-limited by the point spread function of the scintillator
 117 to $(78 \mu\text{m} / M)$ [8]. For each acquisition 10 single x-ray images were integrated and an average flat field beam x-ray
 118 profile was background subtracted as well as a darkfield image. Clusters of hot pixels, due to bremsstrahlung, were

119 removed using an adapted median filter, taking into account that bremsstrahlung affects multiple pixels.

120 **3. Industrial Applications**

121 **3.1. Dimensional XCT**

122 Accurate metrology is a critical aspect of the manufacturing process to confirm that industrial components meet the
123 required tolerances. This is particularly important for parts produced by AM, which have complicated internal structure
124 that must be imaged in a non-destructive way. As an emerging technology, there is a need for new approaches to quality
125 control and the definition of industry standards ⁴.

126 Typical lab-based x-ray machines consisting of a cone beam have a plethora of measurement uncertainties in the
127 scanning procedure. These include variations in operator selected parameters; geometric alignment of the system from
128 the source, detector, and manipulator; and the environment [22]. Post-acquisition, the typical Feldkamp algorithm
129 (FDK) [23] reconstruction introduces further error including approximations from the cone-beam. In an effort to assess
130 the measurement uncertainty in industrial XCT, there have been studies to understand the impact of various parameters
131 and to evaluate performance [24–27]. Results from the entire process carried out on different machines in different
132 locations have also been compared to assess consistency, as reported in numerous round robin tests [28–30].

133 An image using the laser-betatron source of a plastic test object produced for performance verification is shown
134 in Fig. 2 (b). These samples are made with a number of representative geometries designed to test the dimensional
135 measurement accuracy of x-ray imaging systems. Dimensions such as sphere diameter, internal/external diameters of
136 cylinders, centre-to-centre and plane-to-plane distances are typical examples of features that are assessed. In Fig. 2 (a),
137 a tomographic reconstruction of the sample is shown where these distances are evident in a 3D context. The accuracy
138 and uncertainty of such a measurement is intrinsically linked to the quantity and quality of the data that can be captured.
139 The radiograph displays exceptional sharpness with minimal noise due to the small source size and high photon count.
140 This level of fidelity could potentially produce an unrivalled maximal permissible error across all measurements with
141 sufficient radiographs and a high level of geometric calibration. The near-parallelism of the laser-betatron x-ray beam is
142 beneficial as this limits imaging artefacts arising from cone beams. Additionally, the ability to tune the x-ray spectrum
143 to higher energies would allow highly penetrating XCT of AM products made with dense materials such as super-alloys
144 used in the automotive and aerospace sectors.

145 **3.2. Battery technologies**

146 Better understanding of electrochemical processes is essential to guide innovative product design enabling the
147 transition to low-carbon technologies ⁵. The manufacture of Li-batteries is in a constant state of development with

⁴amnationalstrategy.uk

⁵gov.uk/government/publications/clean-growth-strategy

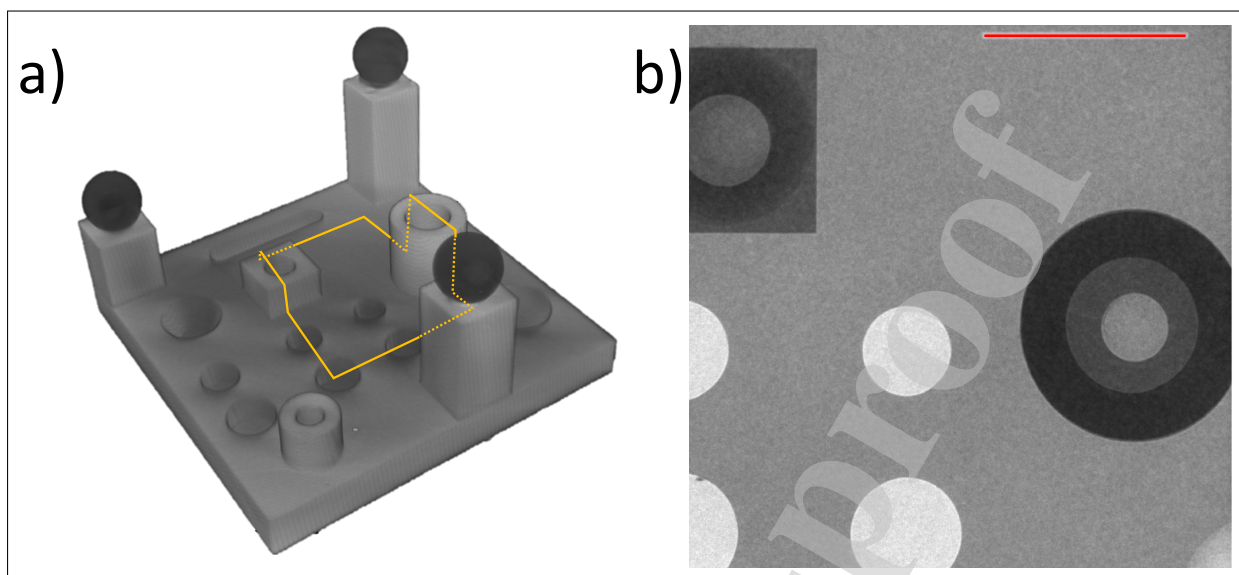


Figure 2: Plastic test object with varying sphere diameters, external/internal diameters of cylinders, and plane to plane distances produced for XCT performance verification. (a) tomographic reconstruction using conventional lab x-ray CT (b) radiograph of the test object obtained with the laser-betatron source. The red line indicates 1 cm and the orange rectangle the field of the radiograph.

148 new chemistries regularly being trialled, with assembly lines eventually needing to adapt. New processes are rarely
 149 right-first-time and can result in defects within the cell. While the manufacturing process is iterated, identification of
 150 these problems is paramount not only to maintain optimal performance but also for safety [31]. XCT is being exploited
 151 to investigate these issues but with manufacturing lines creating 6-10 cells per minute, a high speed solution is required
 152 if every cell is to be inspected.

153 The laser-betatron source is well suited to provide rapid NDE of battery components, as shown by the example
 154 image of a pouch cell in Fig. 3 (b). Pouch cells consist of a gel layer, alternating between cathode and anode layers.
 155 The electrodes must be sufficiently separated with no contact between them to avoid shorting, and can also suffer
 156 from other manufacturing defects such as delamination. These individual layers can be observed in a full tomographic
 157 reconstruction such as the one shown in Fig. 3 (a). Another potential site for quality issues is the tab area visible at the
 158 top of the battery. This region is checked as part of a typical inspection process because poor welding of the tabs to
 159 the anode and cathode can result in a defective cell. The radiograph, centred on the tab area, highlights the quality
 160 achievable with the laser-betatron source, with phase enhancement aiding the distinction between components. For
 161 electrodes composed of weakly absorbing materials, such as graphite, phase imaging is necessary to achieve sufficient
 162 contrast [32].

163 Improvements in laser repetition rate will also enable *operando* XCT and time-resolved x-ray absorption spectroscopy
 164 (XAS) to examine the activity of battery cells during charge cycles. These methods allow visualisation of the changes in

Application of Compact Laser-Driven Accelerator X-Ray Sources for Industrial Imaging

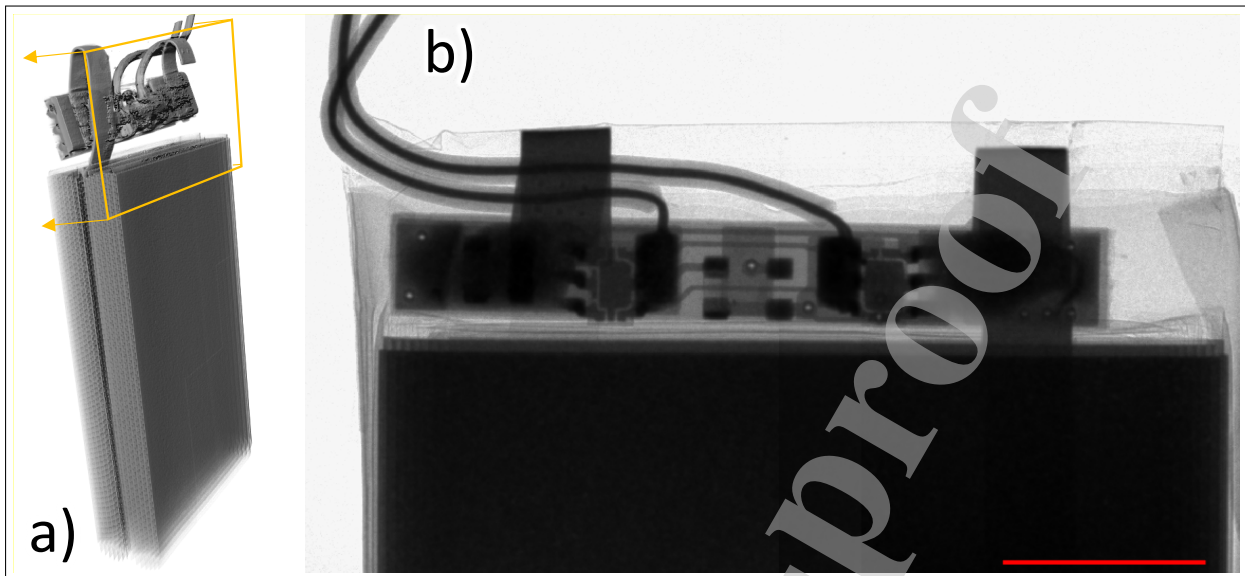


Figure 3: (a) Tomographic reconstruction of a pouch cell obtained using conventional lab x-ray CT. Manufacturing defects can occur such as delamination of layers, improper electrode attachment, and poor welding in the tab area highlighted (b) Front view radiograph of the tab area obtained with the laser-betatron source. The red line indicates 1 cm.

165 microstructure [32, 33] and mapping of lithium concentration [34, 35], important for understanding battery degradation.
 166 However, because of the very high average flux required, such studies can only be currently carried out using synchrotron
 167 light sources. A key advantage of the laser-produced x-ray pulse is its short duration and inherent synchronisation with
 168 the drive laser. The capability to measure ultrafast transitions would be particularly useful for pump-probe investigations
 169 on the femtosecond scale, for example studies of new photovoltaic materials [36]. Laser-betatron XAS measurements
 170 with <100 fs temporal resolution have already been reported [11, 37], demonstrating the suitability of the source for
 171 this application.

172 3.3. Composite manufacturing

173 To meet the huge rise in demand for composite products over a broad range of industries, it is essential to increase
 174 rates and efficiency in composite manufacturing⁶. NDE is commonly used to assess design features, test manufacturing
 175 methods, and inspect the effects of mechanical testing and damage that has occurred over the service lifetime of a part
 176 [38]. Detailed XCT information, along with finite element modelling [39], can improve efficiency through better design,
 177 and the definition of acceptance tolerances.

178 A major concern is the evolution of defects during manufacture. To be able to understand their formation, it is
 179 important to conduct *in-process* XCT to track individual features over time. This was highlighted by a study where
 180 samples were imaged with fast CT scans (7 minute acquisition time) throughout the cure process inside the cabinet of

⁶compositesuk.co.uk/about/industry/uk-composites-strategy

Application of Compact Laser-Driven Accelerator X-Ray Sources for Industrial Imaging

181 an industrial scanner (Nikon *XTH-320*) [40]. The results showed that, although an initial gap between carbon fibre tows
182 filled as the sample heated, small voids emerged that would affect the properties of a finished product. This phenomenon
183 was not detected in other studies using multiple partially cured samples [41], likely because of unavoidable variation in
184 samples [42, 43]. However, the long scan times necessary for high resolution and low noise images present difficulties
185 for studies of fast changing samples. This is particularly true where the research requires distinguishing carbon fibre
186 reinforcements from carbon-based polymer resins. Although this can be achieved with industrial scanners, scan times of
187 order 4 hours preclude this type of in-process XCT study. Synchrotron imaging can be adopted for uninterrupted in-situ
188 studies, including mechanical tests of cured composite [44] and compression [45] and debulk [46] of uncured composite,
189 but this is not a practical solution for regular use by industrial composite manufacturers because of availability and cost
190 constraints.

191 These problems could be overcome by employing laser-driven x-ray sources. As an example, we show in Fig. 4 (b)
192 a radiograph, obtained with the laser-betatron source, of a composite test sample. This was a semi-circular prism cut
193 from a cured cylinder made up from an array of small diameter unidirectional IM7 carbon fibre reinforced epoxy resin
194 matrix rods, embedded in a second epoxy resin. XCT is used to assess the effect of a kink-band failure, initiated by
195 impact and propagated by compressive end loading. This is visible in the tomographic reconstruction shown in Fig. 4
196 (a). The radiograph exhibits good contrast between the carbon fibre and the resin, highlighting the benefit of the x-ray
197 phase enhancement produced with the laser-betatron source. The layers visible in the image are carbon fibre tows that
198 typically have a diameter of order 200 μm . Development of this technology to deliver fast scanning at high resolution
199 would address larger scale challenges, such as imaging consolidation in corners, or inspecting full scale parts while
200 applying heat, vacuum and/or pressure to the part. In this way, quality assurance and control could be performed before
201 the heat and pressure is applied to cure the resin, reducing scrap, and saving energy, cost and time.

202 4. Discussion

203 The demands of state-of-the-art industrial NDE, such as high resolution, fast scan speed and element specific
204 analysis, are difficult to meet with existing x-ray technology. Laser-based radiation sources produced with a plasma
205 accelerator have ideal properties for addressing these challenges. Recent improvements in reliability and repetition rate
206 of high power lasers make it feasible to produce these compact x-ray devices for commercial deployment in industrial
207 environments. At the laser energy used here of 7 J (125 TW laser power), commercial products are available operating
208 at 5 Hz (e.g. Thales *Quark200*; Amplitude *Pulsar*) and would increase the average x-ray flux to above 10^{11} ph s^{-1} .
209 Using diode-pumped solid state technology the repetition rate could be scaled up further [47–50]. Improvements in
210 x-ray beam consistency have been demonstrated by reducing pulse-to-pulse fluctuations in the laser and gas target
211 performance [51] and through studies of the stability of electron injection mechanisms into the accelerator [9]. Using

Application of Compact Laser-Driven Accelerator X-Ray Sources for Industrial Imaging

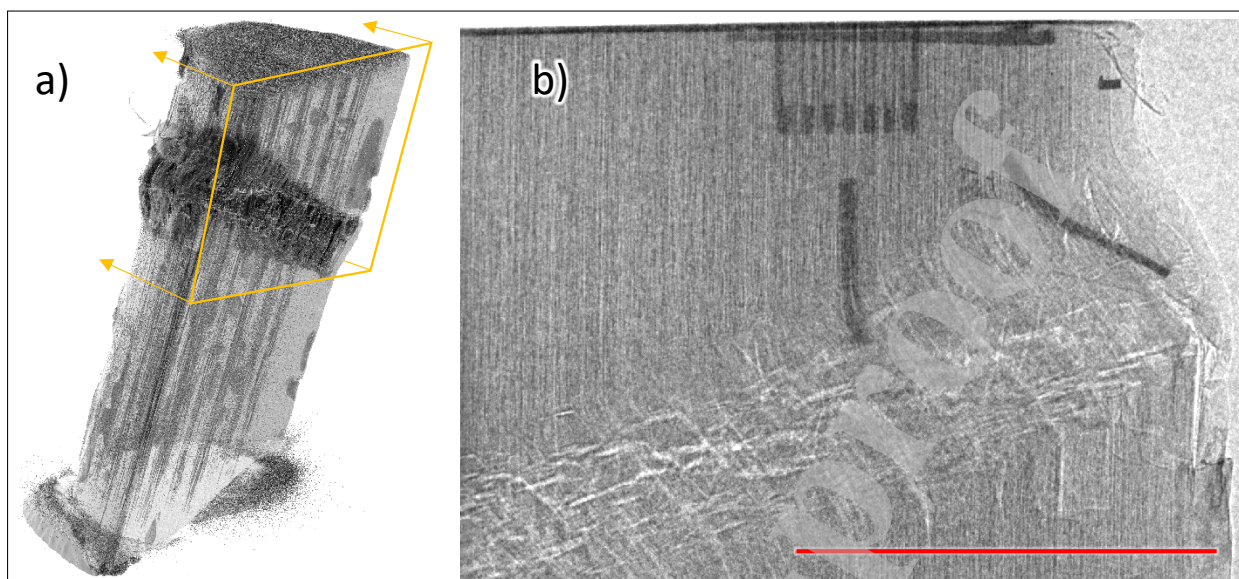


Figure 4: Kink band failure in a composite cylinder initiated by impact and propagated by compressive end loading. (a) tomographic reconstruction obtained using conventional lab x-ray CT (b) radiograph obtained with the laser-betatron source with carbon fibre tows visible. The red line indicates 1 cm.

212 higher power drive lasers [6, 52], the photon energy should be enhanced to the 100s keV to MeV range that will be
 213 needed for inspection of large battery packs and full-scale composite products such as wind turbines, although this also
 214 increases the size and cost of the system. The laser requirements might be relaxed by adapting target design to increase
 215 the betatron photon energy [53].

216 One of the benefits of adopting laser-driven technology is the ability to drive different, synchronised secondary
 217 sources with the same laser. Moderate adaptations to the system can produce other particles that can be utilised for
 218 complementary sub-surface inspection techniques such as neutron imaging [54] and positron annihilation lifetime
 219 spectroscopy [55]. Therefore, a single machine could be used to deliver a powerful inspection capability with multi-
 220 modal, multi-scale imaging.

221 To be viable as a commercial product, considerable R & D effort is needed to ensure robust performance over long
 222 periods and to minimise the size and cost of the system. Product design could be tailored to meet the specific demands
 223 of the end-user, with a range of systems dependent on space and budget constraints. The compact design of modern
 224 high power lasers means that it would also be possible to integrate them into portable devices [56]. An important
 225 consideration is the radiation shielding necessary for the electron beam. In an industrial environment this could be
 226 constructed in a similar way to free-electron laser and synchrotron facilities where the electron beam is deflected into a
 227 heavily shielded beam dump in the ground while the x-ray beam propagates into an end-station with relatively light
 228 shielding.

229 Although a product based on this technology would be more costly and complex than conventional x-ray machines,

Application of Compact Laser-Driven Accelerator X-Ray Sources for Industrial Imaging

230 it would offer advanced NDE tools that are currently not available in industrial or lab-based settings. In particular,
 231 micron-scale resolution tomography with fast scan speed, and ultrafast x-ray absorption spectroscopy could be applied
 232 to in situ inspection and product development. For example, using a laser operating at 100 Hz, high frame rate imaging
 233 of metre-scale objects should be possible at less than 1 minute per square metre. Hard x-ray chemical tomography
 234 could also be conducted following the methods used on XAS synchrotron beamlines [57].

235 5. Acknowledgements

236 The authors thank the staff of the Central Laser Facility and the Science and Technology Facilities Council (STFC)
 237 Technology department for assistance with the experiment, and acknowledge helpful discussions with Ian Sinclair and
 238 his team at the μ -VIS X-Ray Imaging Centre; Nick Brierley at the Manufacturing Technology Centre; Wenjuan Sun
 239 and Stephen Brown at the National Physical Laboratory. Authors from the National Composites Centre (NCC) and
 240 Warwick Manufacturing Group (WMG) thank the High Value Manufacturing Catapult for support.

241 The John Adams Institute acknowledges support by STFC [ST/P002021 /1] and by the EU Horizon 2020 research
 242 and innovation programme grant No. 653782; CT was supported by an Engineering and Physical Sciences Research
 243 Council (EPSRC) Innovation Fellowship grant [EP/S001379/1]; LRP acknowledges support from EPSRC through the
 244 Centre for Doctoral Training in Composites Manufacture [EP/K50323X/1] and by the NCC. The TESCAN UniTom
 245 XL machine used for the CT scan in Fig. 2 and Fig. 3 was funded by EPSRC Strategic Equipment 'High Speed
 246 CT' [EP/S010076/1]. The Nikon XTH-320 machine used for the CT scan in Fig. 4 was purchased under the EPSRC
 247 'Atoms to Applications' grant [EP/K035746/1].

248 References

- 249 [1] F. Albert, A. G. R. Thomas, Plasma Physics and Controlled Fusion vol 1, Plasma Phys. Control. Fusion 58 (103001).
 250 doi:10.1088/0741-3335/58/10/103001.
 251 URL [http://iopscience.iop.org/](http://iopscience.iop.org/article/10.1088/0741-3335/58/10/103001/pdf)
 252 [http://iopscience.iop.org/](http://iopscience.iop.org/article/10.1088/0741-3335/58/10/103001/pdf)
 253 [article/10.1088/0741-3335/57/6/065008/pdf](http://iopscience.iop.org/article/10.1088/0741-3335/57/6/065008/pdf)
- 254 [2] K. Poder, M. Tamburini, G. Sarri, A. D. Piazza, S. Kuschel, C. D. Baird, K. Behm, S. Bohlen, J. M. Cole, D. J. Corvan, M. Duff, E. Gerstmayr,
 255 C. H. Keitel, K. Krushelnick, S. P. D. Mangles, P. McKenna, C. D. Murphy, Z. Najmudin, C. P. Ridgers, G. M. Samarin, D. R. Symes, A. G. R.
 256 Thomas, J. Warwick, M. Zepf, Experimental Signatures of the Quantum Nature of Radiation Reaction in the Field of an Ultraintense Laser,
 257 Physical Review X 8. doi:10.1103/PhysRevX.8.031004.
- 258 [3] A. Rousse, K. Ta Phuoc, R. Shah, A. Pukhov, E. Lefebvre, V. Malka, S. Kiselev, F. Burgy, J. P. Rousseau, D. Umstadter, D. Hulin, Production
 259 of a keV X-ray beam from synchrotron radiation in relativistic laser-plasma interaction, Physical Review Letters 93 (13). doi:10.1103/
 260 PhysRevLett.93.135005.
 261 URL <https://journals.aps.org/prl/pdf/10.1103/PhysRevLett.93.135005>
- 262 [4] S. Kneip, C. McGuffey, J. L. Martins, S. F. Martins, C. Bellei, V. Chvykov, F. Dollar, R. A. Fonseca, C. Huntington, G. Kalintchenko,

Application of Compact Laser-Driven Accelerator X-Ray Sources for Industrial Imaging

- 262 A. Maksimchuk, S. P. D. Mangles, T. Matsuoka, S. R. Nagel, C. A. J. Palmer, J. Schreiber, K. T. Phuoc, A. G. R. Thomas, V. Yanovsky,
263 L. O. Silva, K. Krushelnick, Z. Najmudin, Bright spatially coherent synchrotron X-rays from a table-top source, *Nature Physics* 6 (12) (2010)
264 980–983. doi:10.1038/nphys1789.
265 URL <http://www.nature.com/doi/10.1038/nphys1789>
- [5] E. Esarey, B. A. Shadwick, P. Catravas, W. P. Leemans, Synchrotron radiation from electron beams in plasma-focusing channels, *Physical*
266 *Review E - Statistical, Nonlinear, and Soft Matter Physics* 65 (5) (2002) 1–15. doi:10.1103/PhysRevE.65.056505.
267
- [6] A. G. Thomas, Scalings for radiation from plasma bubbles, *Physics of Plasmas* 17 (5). doi:10.1063/1.3368678.
268 URL <https://doi.org/10.1063/1.3368678><http://aip.scitation.org/toc/php/17/5>
269
- [7] J. M. Cole, J. C. Wood, N. C. Lopes, K. Poder, R. L. Abel, S. Alatabi, J. S. J. Bryant, A. Jin, S. Kneip, K. Mecseki, S. Parker, D. R. Symes,
270 M. A. Sandholzer, S. P. D. Mangles, Z. Najmudin, Tomography of human trabecular bone with a laser-wakefield driven x-ray source, *Plasma*
271 *Physics and Controlled Fusion* 58 (1) (2016) 014008. doi:10.1088/0741-3335/58/1/014008.
272 URL <http://iopscience.iop.org/article/10.1088/0741-3335/58/1/014008/pdf><http://stacks.iop.org/0741-3335/58/i=1/a=014008?key=crossref.4d5ab1142b28c565d26013c3142f828e>
273
274
- [8] J. M. Cole, D. R. Symes, N. C. Lopes, J. C. Wood, K. Poder, S. Alatabi, S. W. Botchway, P. S. Foster, S. Gratton, S. Johnson, C. Kamperidis,
275 O. Kononenko, M. De Lazzari, C. A. J. Palmer, D. Rusby, J. Sanderson, M. Sandholzer, G. Sarri, Z. Szoke-Kovacs, L. Teboul, J. M. Thompson,
276 J. R. Warwick, H. Westerberg, M. A. Hill, D. P. Norris, S. P. D. Mangles, Z. Najmudin, High-resolution μ CT of a mouse embryo using a
277 compact laser-driven X-ray betatron source., *Proceedings of the National Academy of Sciences of the United States of America* 115 (25) (2018)
278 6335–6340. doi:10.1073/pnas.1802314115.
279
- [9] A. Döpp, B. Mahieu, A. Lifschitz, C. Thaury, A. Doche, E. Guillaume, G. Grittani, O. Lundh, M. Hansson, J. Gautier, M. Kozlova, J. P. Goddet,
280 P. Rousseau, A. Tafzi, V. Malka, A. Rousse, S. Corde, K. Ta Phuoc, Stable femtosecond X-rays with tunable polarization from a laser-driven
281 accelerator, *Light: Science & Applications* 6 (11) (2017) e17086–e17086. doi:10.1038/lsa.2017.86.
282 URL <http://dx.doi.org/10.1038/lsa.2017.86>
283
- [10] K. Ta Phuoc, R. Fitour, A. Tafzi, T. Garl, N. Artemiev, R. Shah, F. Albert, D. Boschetto, A. Rousse, D. E. Kim, A. Pukhov, V. Seredov,
284 I. Kostyukov, Demonstration of the ultrafast nature of laser produced betatron radiation, *Physics of Plasmas* 14 (8). doi:10.1063/1.2754624.
285 URL <https://doi.org/10.1063/1.2754624><http://aip.scitation.org/toc/php/14/8>
286
- [11] B. Mahieu, N. Jourdain, K. Ta Phuoc, F. Dorchie, J.-P. Goddet, A. Lifschitz, P. Renaudin, L. Lecherbourg, Probing warm dense matter
287 using femtosecond X-ray absorption spectroscopy with a laser-produced betatron source, *Nature Communications* 9 (1) (2018) 3276. doi:
288 10.1038/s41467-018-05791-4.
289 URL <http://www.nature.com/articles/s41467-018-05791-4>
290
- [12] J. Wenz, S. Schleede, K. Khrennikov, M. Bech, P. Thibault, M. Heigoldt, F. Pfeiffer, S. Karsch, Quantitative X-ray phase-contrast microtomogra-
291 phy from a compact laser-driven betatron source, *Nature Communications* 6 (May) (2015) 1–6. arXiv:0411070, doi:10.1038/ncomms8568.
292 URL <http://dx.doi.org/10.1038/ncomms8568>
293
- [13] A. Döpp, L. Hehn, J. Götzfried, J. Wenz, M. Gilljohann, H. Ding, S. Schindler, F. Pfeiffer, S. Karsch, Quick x-ray microtomography using a
294 laser-driven betatron source, *Optica* 5 (2) (2018) 199. doi:10.1364/OPTICA.5.000199.
295 URL <https://www.osapublishing.org/abstract.cfm?URI=optica-5-2-199>
296
- [14] J. C. Wood, D. J. Chapman, K. Poder, N. C. Lopes, M. E. Rutherford, T. G. White, F. Albert, K. T. Behm, N. Booth, J. S. Bryant, P. S. Foster,
297 S. Glenzer, E. Hill, K. Krushelnick, Z. Najmudin, B. B. Pollock, S. Rose, W. Schumaker, R. H. Scott, M. Sherlock, A. G. Thomas, Z. Zhao, D. E.
298 Eakins, S. P. Mangles, Ultrafast Imaging of Laser Driven Shock Waves using Betatron X-rays from a Laser Wakefield Accelerator, *Scientific*
299

Application of Compact Laser-Driven Accelerator X-Ray Sources for Industrial Imaging

- 300 Reports 8 (1). arXiv:1802.02119, doi:10.1038/s41598-018-29347-0.
- 301 [15] M. Vargas, W. Schumaker, Z.-H. He, K. Behm, V. Chvykov, B. Hou, K. Krushelnick, A. Maksimchuk, J. A. Nees, V. Yanovsky, Z. Zhao,
302 A. G. R. Thomas, X-ray phase contrast imaging of additive manufactured structures using a laser wakefield accelerator, *Plasma Physics and*
303 *Controlled Fusion* 61 (5) (2019) 54009. doi:10.1088/1361-6587/ab0e4f.
304 URL <https://doi.org/10.1088/1361-6587/ab0e4f>
- 305 [16] A. E. Hussein, N. Senabulya, Y. Ma, M. J. Streeter, B. Kettle, S. J. Dann, F. Albert, N. Bourgeois, S. Cipiccia, J. M. Cole, O. Finlay, E. Gerstmayr,
306 I. G. González, A. Higginbotham, D. A. Jaroszynski, K. Falk, K. Krushelnick, N. Lemos, N. C. Lopes, C. Lumsdon, O. Lundh, S. P. Mangles,
307 Z. Najmudin, P. P. Rajeev, C. M. Schlepütz, M. Shahzad, M. Smid, R. Spesyvtsev, D. R. Symes, G. Vieux, L. Willingale, J. C. Wood, A. J.
308 Shahani, A. G. Thomas, Laser-wakefield accelerators for high-resolution X-ray imaging of complex microstructures, *Scientific Reports* 9 (1).
309 doi:10.1038/s41598-019-39845-4.
- 310 [17] S. Kneip, C. McGuffey, F. Dollar, M. S. Bloom, V. Chvykov, G. Kalintchenko, K. Krushelnick, A. Maksimchuk, S. P. Mangles, T. Matsuoka,
311 Z. Najmudin, C. A. Palmer, J. Schreiber, W. Schumaker, A. G. Thomas, V. Yanovsky, X-ray phase contrast imaging of biological specimens
312 with femtosecond pulses of betatron radiation from a compact laser plasma wakefield accelerator, *Applied Physics Letters* 99 (9) (2011) 1–4.
313 doi:10.1063/1.3627216.
- 314 [18] M. Stampanoni, A. Groso, A. Isenegger, G. Mikuljan, Q. Chen, A. Bertrand, S. Henein, R. Betemps, U. Frommherz, P. Böhler, D. Meister,
315 M. Lange, R. Abela, Trends in synchrotron-based tomographic imaging: the SLS experience, in: *Developments in X-Ray Tomography V*, Vol.
316 6318, 2006, pp. 63180M–63180M–14. doi:10.1117/12.679497.
317 URL <http://dx.doi.org/10.1117/12.679497>[http://proceedings.spiedigitallibrary.org/data/conferences/spiep/
318 5533/63180m_{_}1.pdf](http://proceedings.spiedigitallibrary.org/data/conferences/spiep/5533/63180m_{_}1.pdf)
- 319 [19] S. Fourmaux, S. Corde, K. T. Phuoc, P. Lassonde, G. Lebrun, S. Payeur, F. Martin, S. Sebban, V. Malka, A. Rousse, J. C. Kieffer, Single
320 shot phase contrast imaging using laser-produced Betatron x-ray beams, *Optics Letters* 36 (13) (2011) 2426. arXiv:1106.4484, doi:
321 10.1364/ol.36.002426.
- 322 [20] C. Thaury, F. Quéré, J.-P. Geindre, A. Levy, T. Ceccotti, P. Monot, M. Bougeard, F. Réau, P. D'Oliveira, P. Audebert, R. Marjoribanks, P. Martin,
323 Plasma mirrors for ultrahigh-intensity optics, *Nature Physics* 3 (6) (2007) 424–429. doi:10.1038/nphys595.
324 URL <http://www.nature.com/nphys/journal/v3/n6/pdf/nphys595.pdf>
- 325 [21] S. Kneip, S. R. Nagel, C. Bellei, N. Bourgeois, A. E. Dangor, A. Gopal, R. Heathcote, S. P. Mangles, J. R. Marquès, A. Maksimchuk, P. M.
326 Nilson, K. T. Phuoc, S. Reed, M. Tzoufras, F. S. Tsung, L. Willingale, W. B. Mori, A. Rousse, K. Krushelnick, Z. Najmudin, Observation of
327 synchrotron radiation from electrons accelerated in a petawatt-laser-generated plasma cavity, *Physical Review Letters* 100 (10) (2008) 1–4.
328 doi:10.1103/PhysRevLett.100.105006.
- 329 [22] J. P. Kruth, M. Bartscher, S. Carmignato, R. Schmitt, L. De Chiffre, A. Weckenmann, Computed tomography for dimensional metrology, *CIRP*
330 *Annals - Manufacturing Technology* 60 (2) (2011) 821–842. doi:10.1016/j.cirp.2011.05.006.
- 331 [23] L. A. Feldkamp, L. C. Davis, J. W. Kress, Practical cone-beam algorithm, *J. Opt. Soc. Am. A* 1 (6) (1984) 612–619.
- 332 [24] R. Schmitt, C. Niggemann, Uncertainty in measurement for x-ray-computed tomography using calibrated work pieces, *Measurement Science*
333 *and Technology* 21 (5). doi:10.1088/0957-0233/21/5/054008.
- 334 [25] J. Kumar, A. Attridge, P. K. Wood, M. A. Williams, Analysis of the effect of cone-beam geometry and test object configuration on the measurement
335 accuracy of a computed tomography scanner used for dimensional measurement (2011). doi:10.1088/0957-0233/22/3/035105.
- 336 [26] P. Müller, J. Hiller, A. Cantatore, L. De Chiffre, A study on evaluation strategies in dimensional X-ray computed tomography by estimation of
337 measurement uncertainties, *International Journal of Metrology and Quality Engineering* 3 (2) (2012) 107–115. doi:10.1051/ijmqe/2012011.

Application of Compact Laser-Driven Accelerator X-Ray Sources for Industrial Imaging

- 338 URL <http://www.metrology-journal.org/10.1051/ijmqe/2012011>
- 339 [27] J. Hiller, M. Maisl, L. M. Reindl, Physical characterization and performance evaluation of an x-ray micro-computed tomography system for
340 dimensional metrology applications, *Measurement Science and Technology* 23 (8). doi:10.1088/0957-0233/23/8/085404.
- 341 [28] S. Carmignato, Accuracy of industrial computed tomography measurements: Experimental results from an international comparison, *CIRP*
342 *Annals - Manufacturing Technology* 61 (1) (2012) 491–494. doi:10.1016/j.cirp.2012.03.021.
- 343 [29] J. A. B. Angel, L. De Chiffre, E. Larsen, J. Rasmussen, R. Sobiecki, General rights Inter laboratory comparison on Industrial Computed
344 Tomography CIA-CT comparison. Reference Measurements CIA-CT_Reference_Measurements_01 CIA-CT comparison Inter laboratory
345 comparison on Industrial Computed Tomography Reference Measurements List of contents, Tech. Rep. 01, DTU Mechanical Engineering
346 (2013).
- 347 [30] A. Townsend, R. Racasan, R. Leach, N. Senin, A. Thompson, A. Ramsey, D. Bate, P. Woolliams, S. Brown, L. Blunt, An interlaboratory
348 comparison of X-ray computed tomography measurement for texture and dimensional characterisation of additively manufactured parts,
349 *Additive Manufacturing* 23 (2018) 422–432. doi:10.1016/j.addma.2018.08.013.
- 350 [31] M. Loveridge, G. Remy, N. Kourra, R. Genieser, A. Barai, M. Lain, Y. Guo, M. Amor-Segan, M. Williams, T. Amietszajew, M. Ellis, R. Bhagat,
351 D. Greenwood, Looking Deeper into the Galaxy (Note 7), *Batteries* 4 (1) (2018) 3. doi:10.3390/batteries4010003.
352 URL <http://www.mdpi.com/2313-0105/4/1/3>
- 353 [32] P. Pietsch, D. Westhoff, J. Feinauer, J. Eller, F. Marone, M. Stampanoni, V. Schmidt, V. Wood, Quantifying microstructural dynamics and
354 electrochemical activity of graphite and silicon-graphite lithium ion battery anodes, *Nature Communications* 7 (1) (2016) 12909. doi:
355 10.1038/ncomms12909.
356 URL <http://www.nature.com/articles/ncomms12909>
- 357 [33] M. Ebner, F. Marone, M. Stampanoni, V. W. Science, undefined 2013, Visualization and quantification of electrochemical and mechanical
358 degradation in Li ion batteries, science.sciencemag.org.
359 URL <http://science.sciencemag.org/content/342/6159/716.short>
- 360 [34] L. Nowack, D. Grolimund, V. Samson, F. Marone, V. Wood, Rapid Mapping of Lithiation Dynamics in Transition Metal Oxide Particles with
361 Operando X-ray Absorption Spectroscopy, *Scientific Reports* 6 (1) (2016) 21479. doi:10.1038/srep21479.
362 URL <http://www.nature.com/articles/srep21479>
- 363 [35] J. Wang, Y.-c. Karen Chen-Wiegart, C. Eng, Q. Shen, J. Wang, Visualization of anisotropic-isotropic phase transformation dynamics in battery
364 electrode particles, *Nature Communications* 7 (1) (2016) 12372. doi:10.1038/ncomms12372.
365 URL <http://www.nature.com/articles/ncomms12372>
- 366 [36] Y. Uemura, D. Kido, A. Koide, Y. Wakisaka, Y. Niwa, S. Nozawa, K. Ichianagi, R. Fukaya, S.-i. Adachi, T. Katayama, T. Togashi, S. Owada,
367 M. Yabashi, K. Hatada, A. Iwase, A. Kudo, S. Takakusagi, T. Yokoyama, K. Asakura, Capturing local structure modulations of photoexcited
368 BiVO₄ by ultrafast transient XAFS, *Chemical Communications* 53 (53) (2017) 7314–7317. doi:10.1039/C7CC02201H.
369 URL <http://xlink.rsc.org/?DOI=C7CC02201H>
- 370 [37] B. Kettle, E. Gerstmayr, M. Streeter, F. Albert, R. Baggott, N. Bourgeois, J. Cole, S. Dann, K. Falk, I. Gallardo González, A. Hussein,
371 N. Lemos, N. Lopes, O. Lundh, Y. Ma, S. Rose, C. Spindloe, D. Symes, M. Šmíd, A. Thomas, R. Watt, S. Mangles, Single-Shot Multi-keV
372 X-Ray Absorption Spectroscopy Using an Ultrashort Laser-Wakefield Accelerator Source, *Physical Review Letters* 123 (25) (2019) 254801.
373 doi:10.1103/PhysRevLett.123.254801.
374 URL <https://link.aps.org/doi/10.1103/PhysRevLett.123.254801>
- 375 [38] S. C. Garcea, Y. Wang, P. J. Withers, X-ray computed tomography of polymer composites, *Composites Science and Technology* 156 (2018)

Application of Compact Laser-Driven Accelerator X-Ray Sources for Industrial Imaging

- 376 305–319. doi:<https://doi.org/10.1016/j.compscitech.2017.10.023>.
- 377 URL <http://www.sciencedirect.com/science/article/pii/S0266353817312460>
- 378 [39] J. P.-H. Belnoue, T. Mesogitis, O. J. Nixon-Pearson, J. Kratz, D. S. Ivanov, I. K. Partridge, K. D. Potter, S. R. Hallett, Understanding and
379 predicting defect formation in automated fibre placement pre-preg laminates, *Composites Part A: Applied Science and Manufacturing* 102
380 (2017) 196–206. doi:[10.1016/J.COMPOSITESA.2017.08.008](https://doi.org/10.1016/J.COMPOSITESA.2017.08.008).
- 381 URL <https://www.sciencedirect.com/science/article/pii/S1359835X17303081>
- 382 [40] L. R. Pickard, K. Smith, J. Kratz, K. Potter, Tracking the Evolution of a Defect, Characteristic of Afp Layup, During Cure With in-Process
383 Micro-Ct Scanning, in: *21st International Conference on Composite Materials*, 2017.
- 384 URL <http://www.bristol.ac.uk/composites/>
- 385 [41] L. R. Pickard, *Towards Efficient Composites Manufacture Through In-Process Monitoring and Knowledge Management*, Dissertation. University
386 of Bristol.
- 387 URL <https://bris.on.worldcat.org/oclc/1126650182>
- 388 [42] T. Centea, P. Hubert, Measuring the impregnation of an out-of-autoclave prepreg by micro-CT, *Composites Science and Technology* 71 (5)
389 (2011) 593–599. doi:<https://doi.org/10.1016/j.compscitech.2010.12.009>.
- 390 URL <http://www.sciencedirect.com/science/article/pii/S026635381000477X>
- 391 [43] L. Serrano, *Systèmes époxyde- Cuisson hors autoclave et basse température*, Ph.D. thesis, Université de Toulouse (2018).
- 392 [44] A. E. Scott, M. Mavrogordato, P. Wright, I. Sinclair, S. M. Spearing, In situ fibre fracture measurement in carbon fibre epoxy laminates using
393 high resolution computed tomography, *Composites Science and Technology* 71 (12) (2011) 1471–1477. doi:[https://doi.org/10.1016/
394 j.compscitech.2011.06.004](https://doi.org/10.1016/j.compscitech.2011.06.004).
- 395 URL <http://www.sciencedirect.com/science/article/pii/S0266353811002090>
- 396 [45] D. F. Sentsis, L. Orgéas, P. J. J. Dumont, S. R. du Roscoat, M. Sager, P. Latil, 3D in situ observations of the compressibility and pore transport in
397 Sheet Moulding Compounds during the early stages of compression moulding, *Composites Part A: Applied Science and Manufacturing* 92
398 (2017) 51–61. doi:<https://doi.org/10.1016/j.compositesa.2016.10.031>.
- 399 URL <http://www.sciencedirect.com/science/article/pii/S1359835X1630358X>
- 400 [46] J. e. a. Thompson, *Micro-Computed Tomographic Synchrotron Techniques for Non-destructive Testing of out of Autoclave Composite*
401 *Materials*, in: *Design, manufacturing and applications of composites*, in: *Tenth Joint Canada-Japan Workshop on Composites*, 2014, pp.
402 331–335.
- 403 [47] P. Mason, M. Divoký, K. Ertel, J. Pilař, T. Butcher, M. Hanuš, S. Banerjee, J. Phillips, J. Smith, M. D. Vido, A. Lucianetti, C. Hernandez-
404 Gomez, C. Edwards, T. Mocek, J. Collier, Kilowatt average power 100 J-level diode pumped solid state laser, *Optica* 4 (4) (2017) 438–439.
405 doi:[10.1364/OPTICA.4.000438](https://doi.org/10.1364/OPTICA.4.000438).
- 406 URL <https://www.osapublishing.org/abstract.cfm?uri=optica-4-4-438>[https://www.osapublishing.org/optica/
407 abstract.cfm?uri=optica-4-4-438](https://www.osapublishing.org/optica/abstract.cfm?uri=optica-4-4-438)[https://www.osapublishing.org/viewmedia.cfm?uri=optica-4-4-438{&seq=0](https://www.osapublishing.org/viewmedia.cfm?uri=optica-4-4-438&seq=0)
- 408 [48] C. L. Haefner, A. Bayramian, S. Betts, R. Bopp, S. Buck, J. Cupal, M. Drouin, A. Erlandson, J. Horáček, J. Horner, J. Jarboe, K. Kasl, D. Kim,
409 E. Koh, L. Koubíková, W. Maranville, C. Marshall, D. Mason, J. Menapace, P. Miller, P. Mazurek, A. Naylon, J. Novák, D. Peceli, P. Rosso,
410 K. Schaffers, E. Sistrunk, D. Smith, T. Spinka, J. Stanley, R. Steele, C. Stolz, T. Suratwala, S. Telford, J. Thoma, D. VanBlarcom, J. Weiss,
411 P. Wegner, High average power, diode pumped petawatt laser systems: a new generation of lasers enabling precision science and commercial
412 applications, in: G. Korn, L. O. Silva (Eds.), *Proceedings Volume 10241, Research Using Extreme Light: Entering New Frontiers with*
413 *Petawatt-Class Lasers III*, Vol. 10241, International Society for Optics and Photonics, 2017, p. 1024102. doi:[10.1117/12.2281050](https://doi.org/10.1117/12.2281050).

Application of Compact Laser-Driven Accelerator X-Ray Sources for Industrial Imaging

- 414 URL <http://proceedings.spiedigitallibrary.org/proceeding.aspx?doi=10.1117/12.2281050>
- 415 [49] L. Gizzi, P. Koester, L. Labate, F. Mathieu, Z. Mazzotta, G. Toci, M. Vannini, A viable laser driver for a user plasma accelerator, *Nuclear*
416 *Instruments and Methods in Physics Research Section A: Accelerators, Spectrometers, Detectors and Associated Equipment* 909 (2018) 58–66.
417 doi:10.1016/j.nima.2018.02.089.
418 URL <https://linkinghub.elsevier.com/retrieve/pii/S0168900218302717>
- 419 [50] W. P. Leemans, Report of Workshop on Laser Technology for k-BELLA and Beyond, Workshop held at Lawrence Berkeley National Laboratory.
- 420 [51] N. Delbos, C. Werle, I. Dornmair, T. Eichner, L. Hübner, S. J alas, S. W. Jolly, M. Kirchen, V. Leroux, P. Messner, M. Schnepf, M. Trunk,
421 P. A. Walker, P. Winkler, A. R. Maier, LUX A laser-plasma driven undulator beamline, *Nuclear Instruments and Methods in*
422 *Physics Research, Section A: Accelerators, Spectrometers, Detectors and Associated Equipment* 909 (2018) 318–322. arXiv:1801.07651,
423 doi:10.1016/j.nima.2018.01.082.
- 424 [52] S. Kneip, Z. Najmudin, A. G. R. Thomas, A plasma wiggler beamline for 100 TW to 10 PW lasers, *High Energy Density Physics* 8 (2) (2012)
425 133–140. doi:<https://doi.org/10.1016/j.hedp.2011.12.001>.
426 URL <http://www.sciencedirect.com/science/article/pii/S157418181100111X>
- 427 [53] J. Ferri, S. Corde, A. Döpp, A. Lifschitz, A. Doche, C. Thauray, K. Ta Phuoc, B. Mahieu, I. A. Andriyash, V. Malka, X. Davoine, High-
428 Brilliance Betatron γ -Ray Source Powered by Laser-Accelerated Electrons, *Physical Review Letters* 120 (25) (2018) 254802. doi:10.1103/
429 *PhysRevLett*.120.254802.
430 URL <https://link.aps.org/doi/10.1103/PhysRevLett.120.254802>
- 431 [54] E. Lehmann, D. Mannes, A. Kaestner, C. Grünzweig, Recent Applications of Neutron Imaging Methods, *Physics Procedia* 88 (September 2016)
432 (2017) 5–12. doi:10.1016/j.phpro.2017.06.055.
433 URL <http://dx.doi.org/10.1016/j.phpro.2017.06.055>
- 434 [55] M. Butterling, W. Anwand, T. E. Cowan, A. Hartmann, M. Jungmann, R. Krause-Rehberg, A. Krille, A. Wagner, Gamma-induced Positron
435 Spectroscopy (GiPS) at a superconducting electron linear accelerator, *Nuclear Instruments and Methods in Physics Research, Section B: Beam*
436 *Interactions with Materials and Atoms* 269 (22) (2011) 2623–2629. doi:10.1016/j.nimb.2011.06.023.
437 URL <http://dx.doi.org/10.1016/j.nimb.2011.06.023>
- 438 [56] H. Wille, M. Rodriguez, J. Kasparian, D. Mondelain, J. Yu, A. Mysyrowicz, R. Sauerbrey, J. P. Wolf, L. Wöste, Teramobile: A mobile
439 femtosecond-terawatt laser and detection system, *Eur. Phys. J. AP* 20 (2002) 183–190. doi:10.1051/epjap:2002090.
440 URL <http://www.teramobile.org/publications/AP01224.pdf>
- 441 [57] S. W. T. Price, K. Ignatyev, K. Geraki, M. Basham, J. Filik, N. T. Vo, P. T. Witte, A. M. Beale, J. F. W. Mosselmans, Chemical imaging
442 of single catalyst particles with scanning μ -XANES-CT and μ -XRF-CT, *Physical Chemistry Chemical Physics* 17 (1) (2015) 521–529.
443 doi:10.1039/C4CP04488F.
444 URL <http://xlink.rsc.org/?DOI=C4CP04488F>

CRedit author statement

All the authors contributed: Conceptualization, Methodology, Writing- Original draft preparation, Writing- Reviewing and Editing to this work.

J.-N. Gruse

M. J. V. Streeter

C. Thornton

C. D. Armstrong

C. D. Baird

N. Bourgeois

S. Cipiccia

O. J. Finlay

C. D. Gregory

Y. Katzir

N. C. Lopes

S. P. D. Mangles

Z. Najmudin

D. Neely

L. R. Pickard

K. D. Potter

P. P. Rajeev

D. R. Rusb

C. I. D. Underwood

J. M. Warnett

M. A. Williams

J. C. Wood

C. D. Murphy

C. M. Brenner

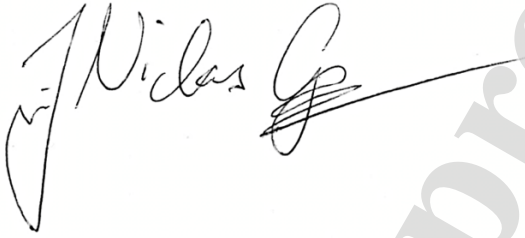
D. R. Symes

Declaration of interests

The authors declare that they have no known competing financial interests or personal relationships that could have appeared to influence the work reported in this paper.

The authors declare the following financial interests/personal relationships which may be considered as potential competing interests:

Jan-Niclas Gruse

A handwritten signature in black ink, appearing to read 'Jan-Niclas Gruse', is enclosed within a rectangular black border. The signature is written in a cursive style with a prominent initial 'J' and 'N'.

Journal Pre-proof